

Ice Flow of Glacier AX010 in the Nepal Himalaya

Koichi IKEGAMI¹ and Yutaka AGETA²

¹ Hayashi Denko Co. Ltd., 6-5-5, Honkomagome, Bunkyo-ku, Tokyo, 113 Japan

² Water Research Institute, Nagoya University, Nagoya, 464-01 Japan

(Received November 27, 1990; Revised manuscript received January 19, 1991)

Abstract

Ice flow surveys of a small glacier were carried out in east Nepal as part of a comprehensive study of the summer-accumulation type glacier from May, 1978 to September, 1979. Observational results of horizontal flow and emergence-submergence flow are described. Then, ice flux and ice thickness are calculated from the ice flow data. Changes of ice thickness are obtained from emergence velocity and mass balance; the area-averaged value for the whole glacier shows thinning of the glacier (0.52 m in water equivalent from Sep., 1978 to Sep., 1979). This coincides well with the observed net balance in the area-average (-0.53 m).

1. Introduction

Glaciological observations were carried out in the Shorong region, east Nepal in 1978 as part of the Glaciological Expedition of Nepal (Higuchi, 1980). Glacier AX010 (glacier number in the inventory by Higuchi *et al.*, 1978), which is the southernmost glacier in the drainage of Dudh Kund Khola (river), was selected for the present study.

The Shorong region is located at the southern front of the Nepal Himalaya where the climate is influenced by the Indian summer monsoon to a great extent. 70-80 % of annual precipitation occurs in the summer season, from June to September. Therefore, accumulation and ablation of glaciers occur simultaneously in the summer monsoon season and mass exchange is quite small in the other seasons. In 1978, total precipitation of 1427 mm was recorded at the terminus of Glacier AX010 at an altitude of 4958 m during the summer season (June 10 to September 25).

Observations were conducted from the viewpoint of investigating the relations between such a monsoon climate and mass balance characteristics of the glacier. Measurements of mass balance, ice temperature of surface layers, heat balance at the glacier surface, general meteorological elements and ice flow were made from May to September, 1978. Results

except ice flow measurements have already been reported by Ageta *et al.* (1980) for mass balance, by Ohata and Higuchi (1980) for heat balance, by Ohata *et al.* (1980) for albedo of the glacier surface and by Tanaka *et al.* (1980) for ice temperature.

When one of the authors (Ageta) visited the glacier twice, in March-April and in September, 1979, some observations including re-surveying of the stake positions were carried out. On the basis of those results, the mass balance of the glacier through 1978 and 1979 was reported by Ageta (1983).

In this paper, horizontal flow and emergence-submergence flow are described on the basis of observations made in 1978 and 1979. And ice flux, ice thickness and the thickness change are calculated from the results of ice flow and mass balance observations.

2. Methods

2.1. Observations

The location of Glacier AX010 is shown in Fig. 1. The glacier originates under a rock peak 5381 m in altitude and terminates in a pond at 4952 m (Figs. 1 and 2). The glacier is 1.7 km long along the center line of the glacier and has an area of 0.57 km². Since small glaciers are sensitive to short range climatic

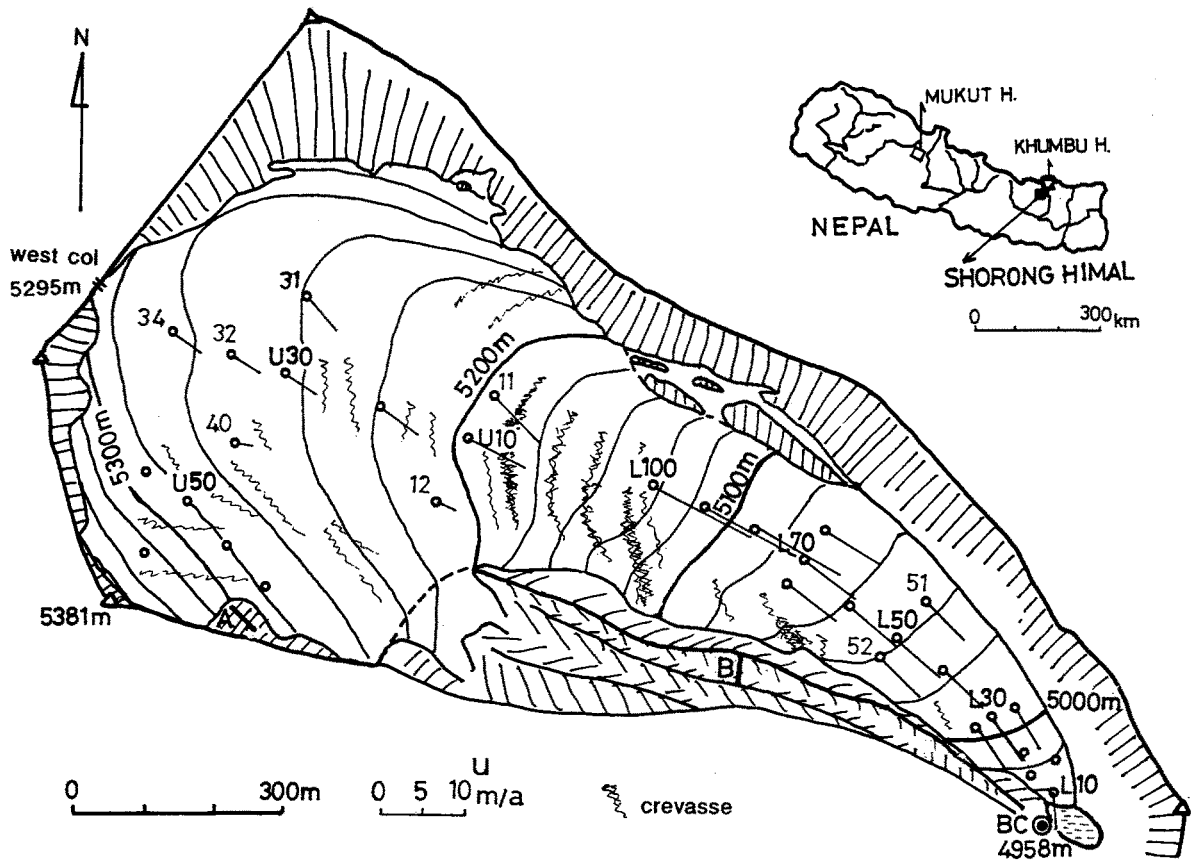


Fig. 1. Topography and distribution of horizontal ice velocities of Glacier AX010 in Shorong Himal. (A: base line of survey for upper stakes, B: that for lower stakes)

variations, this glacier was selected.

For measurement of flow velocities, the positions of stakes were surveyed by triangulation from two base lines established on the rock ridge of the right bank of the glacier, as shown in Fig. 1. Angles were measured with a Wild T-2 theodolite and the lengths of the base lines were determined using a substance bar. Base line A was set for the survey of the stakes at the upper part of the glacier (U-stations) and line B for the lower part (L-stations) with length of 39.73 m and 38.21 m, respectively.

Positions of each stake were measured four times, namely, May 26-June 5 and September 16-18 in 1978, and March 31-April 1 and September 7-10 in 1979. Flow velocities during the three periods were calculated from the displacements of the stakes.

2.2. Calculations

Horizontal flow velocity (u), vertical velocity (w) and azimuth of horizontal velocity (ϕ), which is

measured clockwise from the north, were obtained from the displacement of the stakes. Furthermore, the emergence flow component was calculated as

$$w_E = w + u \cdot \tan \alpha \quad (1)$$

where α is the maximum surface slope.

Flow velocities of L10 and L80 were determined by different methods. At L10, the distance between the stake and a fixed point on the bed rock near the terminus was measured with a tape; then, displacement of the stake was calculated. Since the directions to L80 from the base points for the triangulation survey are close to the direction of the base line, the accuracy of triangulation is insufficient. Consequently, the following method was used to calculate the horizontal velocity. The flow direction was taken to be the direction of the maximum surface slope, and the result of the first triangulation survey was adopted for the initial distance between the stake and the base point. Displacement of the stake was calculated

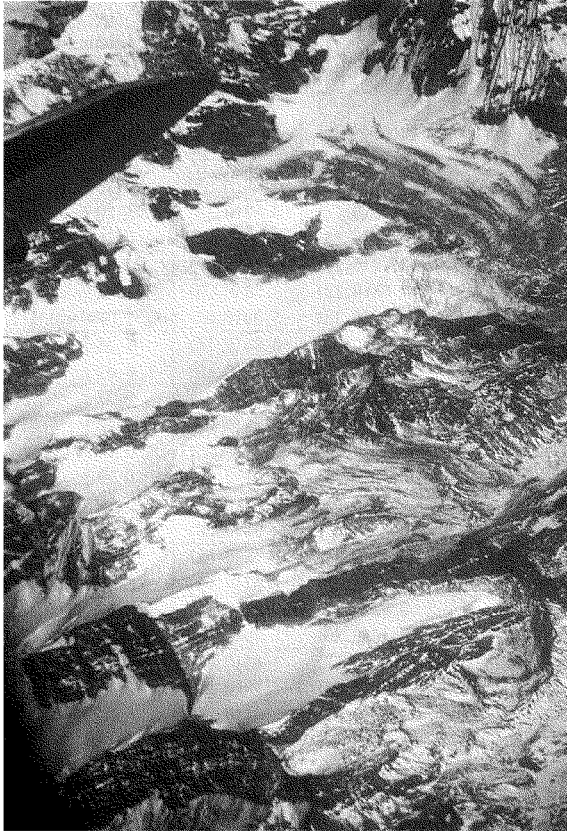


Fig. 2. Air photograph of Glacier AX010 (bottom of picture)

from the above data and the angle between initial direction from the base point to the stake and that at the next surveying time.

Since flow velocities of stakes above an altitude of 5280 m were as small as the magnitude of the measurement error, these data are neglected in this report. Also, results of upper stakes (U10 to U40) from June 4 to September 17 in 1978 are not used because of insufficient accuracy of the survey on June 4.

3. Results

3.1. Surface velocity

Surface horizontal velocities and vertical velocities of each stake are listed in Table 1, and annual horizontal velocities are shown in Fig. 1. Horizontal velocities are less than 10 m/a at most places. This small speed of glacier flow is attributed to the small amount of annual exchange, which is one of characteristics of summer-accumulation type glaciers (Ageta, 1983).

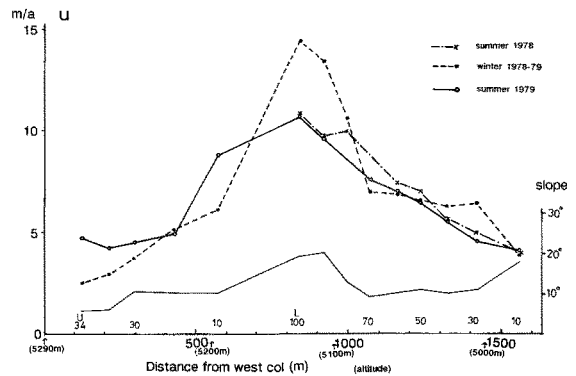


Fig. 3. Horizontal velocities in different seasons and surface slopes along the center line of Glacier AX010

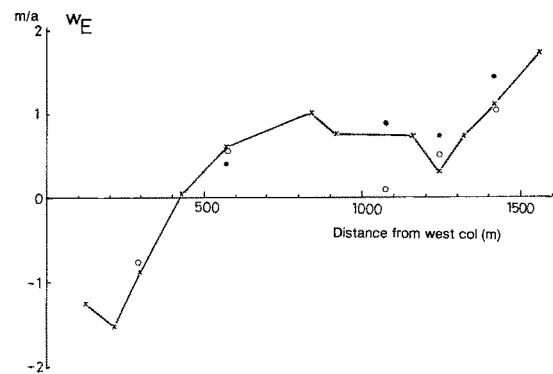


Fig. 4. Emergence velocities of Glacier AX010 from Sep., 1978 to Sep., 1979 (cross: center line, open circle: left bank side, solid circle: right bank side)

Horizontal velocities in different seasons along the center line of the glacier are plotted in Fig. 3 with the surface slope. As seen in Fig. 3, maximum velocity occurs in the steep middle reaches of the glacier. It is interesting that at L30, L90 and L100, velocity in winter is obviously higher than that in summer.

3.2. Emergence velocity

Emergence velocities, w_E , are shown in Table 1 for each stake and plotted as the value obtained from the observation through one balance year from September 1978 to September 1979 in Fig. 4. The emergence velocity goes through zero at a distance of 420 m from the west col, which corresponds to 5220 m in altitude. According to the mass balance observations (Ageta, 1983), the equilibrium line of the glacier in that balance year lay at 5240 m in altitude. Consequently, these results show that emergence velocity is, as would be expected, negative in the accumulation area

Table 1. Horizontal (u), vertical (w) and emergence (w_E) velocities at the surface of Glacier AX 010 in the Nepal Himalaya

| Stake No. (altitude m) | Period | u m/a | w m/a | w_E m/a | ϕ deg | Stake No. (altitude m) | Period | u m/a | w m/a | w_E m/a | ϕ deg |
|---------------------------|--------|------------|-------------|--------------|---------------|---------------------------|----------------|-------------|-------------|--------------|---------------|
| L 10 (4956) | I | 4.08 | -1.25 | 0.09 | 175 | L 80 (5088) | I | 9.99(—) | —(—) | — | 120 |
| | II | 3.88 | 1.19 | 2.46 | 175 | | II | 10.56(—) | —(—) | — | 120 |
| | III | 4.13 | -0.55 | 0.78 | 175 | | IV | 11.08(—) | —(—) | — | 120 |
| | IV | 3.99 | 0.42 | 1.71 | 175 | | L 90 (5113) | I | 9.66(0.11) | -3.85(0.05) | -0.32 |
| L 30 (5007) | I | 4.96(0.13) | 0.37(0.08) | 1.33 | 156 | II | 13.38(0.12) | -3.82(0.13) | 1.30 | 127 | |
| | II | 6.53(0.11) | -0.05(0.12) | 1.20 | 138 | IV | 11.56(0.13) | -3.44(0.04) | 0.76 | 118 | |
| | IV | 5.65(0.08) | 0.02(0.02) | 1.12 | 142 | L 100 (5143) | I | 10.78(0.18) | -2.86(0.07) | 0.86 | 107 |
| L 31 (5008) | I | 5.04(0.12) | 0.15(0.08) | 1.24 | 160 | II | 14.38(0.12) | -3.58(0.03) | 1.41 | 122 | |
| | II | 6.54(0.14) | -0.23(0.10) | 1.17 | 135 | IV | 12.76(0.12) | -3.39(0.05) | 1.00 | 117 | |
| | IV | 5.24(0.10) | -0.05(0.05) | 1.06 | 149 | U 10 (5195) | II | 6.10(0.08) | -0.62(0.10) | 0.46 | 118 |
| L 32 (5004) | I | 4.42(0.17) | 0.66(0.08) | 1.78 | 154 | IV | 7.33(0.08) | -0.68(0.10) | 0.61 | 117 | |
| | II | 6.23(0.10) | 0.13(0.10) | 1.69 | 141 | U 11 (5196) | II | 7.12(0.07) | -0.88(0.07) | 0.37 | 126 |
| | IV | 5.65(0.10) | 0.19(0.05) | 1.60 | 145 | III | 7.39(0.11) | -0.34(0.03) | 0.95 | 144 | |
| L 40 (5023) | I | 5.57(0.11) | 0.06(0.06) | 1.05 | 149 | U 12 (5207) | II | 2.15(0.08) | -0.27(0.05) | 0.24 | 106 |
| | II | 6.31(0.09) | -0.36(0.10) | 0.75 | 130 | III | 1.60(0.05) | -0.07(0.08) | 0.29 | 126 | |
| | IV | 5.96(0.08) | -0.31(0.03) | 0.74 | 134 | U 20 (5219) | II | 5.12(0.08) | -0.67(0.05) | 0.22 | 121 |
| L 50 (5041) | I | 6.99(0.10) | -1.29(0.07) | 0.06 | 136 | III | 4.83(0.07) | -0.96(0.06) | -0.09 | 132 | |
| | II | 6.55(0.07) | -0.77(0.10) | 0.51 | 130 | U 30 (5245) | II | 3.75(0.12) | -1.55(0.05) | -0.82 | 105 |
| | IV | 6.55(0.07) | -0.92(0.02) | 0.34 | 131 | III | 4.52(0.15) | -1.42(0.05) | -0.54 | 138 | |
| L 51 (5043) | I | 6.32(0.12) | -1.00(0.06) | 0.25 | 146 | U 31 (5239) | II | 3.62(0.19) | -1.31(0.05) | -0.69 | 124 |
| | II | 6.14(0.09) | -0.79(0.19) | 0.47 | 127 | III | 5.96(0.20) | -1.20(0.06) | -0.16 | 154 | |
| | IV | 5.88(0.10) | -0.69(0.04) | 0.51 | 135 | U 32 (5256) | II | 2.94(0.18) | -1.83(0.05) | -1.51 | 105 |
| L 52 (5040) | I | 6.40(0.08) | -1.19(0.04) | 0.41 | 137 | III | 4.26(0.24) | -1.73(0.05) | -1.27 | 134 | |
| | II | 6.36(0.05) | -0.67(0.12) | 0.90 | 132 | U 34 (5262) | II | 2.44(0.31) | -1.54(0.05) | -1.38 | 105 |
| | IV | 6.19(0.05) | -0.78(0.05) | 0.77 | 134 | III | 4.87(0.44) | -1.11(0.06) | -0.77 | 144 | |
| L 60 (5059) | I | 7.46(0.08) | -0.60(0.06) | 0.76 | 135 | U 40 (5252) | II | 1.51(0.08) | -0.41(0.04) | -0.14 | 71 |
| | II | 6.87(0.05) | -0.16(0.11) | 1.20 | 127 | III | 1.68(0.12) | -0.63(0.05) | -0.33 | 130 | |
| | IV | 6.89(0.05) | -0.49(0.04) | 0.72 | 130 | | | | | | |
| L 70 (5072) | II | 6.97(0.19) | -0.13(0.12) | 1.15 | 118 | | | | | | |
| | IV | 7.24(—) | —(—) | — | 126 | | | | | | |
| L 71 (5073) | I | 8.46(0.16) | -0.63(0.04) | 0.10 | 135 | | | | | | |
| | II | 7.29(0.07) | -0.23(0.11) | 0.41 | 111 | | | | | | |
| | IV | 7.24(0.07) | -0.56(0.05) | 0.07 | 121 | | | | | | |
| L 72 (5069) | I | 8.31(0.08) | -0.26(0.04) | 1.22 | 134 | | | | | | |
| | II | 6.60(0.04) | 0.23(0.12) | 1.60 | 121 | | | | | | |
| | IV | 6.87(0.04) | 0.11(0.05) | 1.33 | 127 | | | | | | |

Period I : May or Jun.—Sep.,1978

II : Sep.,1978—Mar.or Apr.,1979

III : Mar.or Apr.—Sep.,1979

IV : Sep.,1978—Sep.,1979 (II · III)

ϕ : Horizontal flow direction clockwise from the north

() : Standard deviation of u , w

and positive in the ablation area.

4. Discussions

4.1. Ice flux and thickness

If the emergence velocity is known at the surface of a glacier, the ice flux can be calculated from the equation of continuity applied to a local part of the glacier. This equation is

$$-\Delta Q + \bar{b} \cdot \Delta S_s - \bar{m} \cdot \Delta S_b = \bar{h} \cdot \Delta S_s \quad (2)$$

where ΔQ is the difference ($Q_2 - Q_1$) between ice flux at an upper vertical boundary (Q_1) and that at a lower vertical boundary (Q_2) of a local glacier part in unit time; b , m and h are balance at glacier surface, melting at glacier bed and ice thickness change in unit

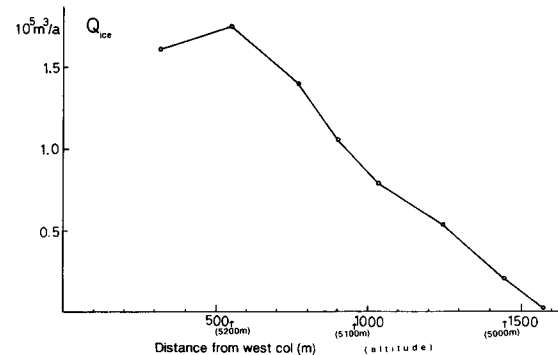


Fig. 5. Ice flux of Glacier AX010 from Sep., 1978 to Sep., 1979

time, respectively. ΔS_s and ΔS_b are surface and sub-surface area, respectively, and bar means averaged value over the area of ΔS_s or ΔS_b .

The rate of ice thickness change can be expressed as

$$\bar{h} \cdot \Delta S_s = (\bar{b} + \bar{w}_E) \Delta S_s - \bar{m} \cdot \Delta S_b \quad (3)$$

where \bar{w}_E is mean value of the emergence velocity. Then, we can obtain the following relation:

$$-\Delta Q = \bar{w}_E \cdot \Delta S_s \quad (4)$$

Ice flux, Q , was calculated every 40 m in altitude using equation (4). Since sufficient flow velocity data were not available above 5280 m, Q through the cross-section at this altitude was assumed to be zero. Because that area is small as seen in Fig. 1 and velocities were also small as mentioned in section 2.2, the error due to such neglect is considered to be small in the calculation of Q .

Amounts of Q (in ice volume) are shown in Fig. 5. Q reaches a maximum of $1.7 \times 10^5 \text{ m}^3/\text{a}$ at an altitude of 5200 m and then decreases almost to zero at the terminus. The altitude of 5200 m where Q shows a maximum coincides nearly with the position of the equilibrium line in the observed balance year.

From the obtained Q , the mean ice thickness, \bar{H} , of the glacier at each cross-section can be calculated from the following relation:

$$Q = \bar{U} \cdot \bar{H} \cdot W \quad (5)$$

where \bar{U} is the velocity averaged over both width and depth and W is surface width. Because velocity distributions with depth are unknown, \bar{H} was computed from the measured surface velocity averaged over only surface width. Since the surface velocity is

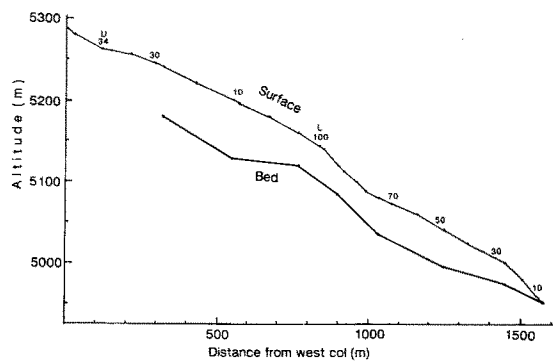


Fig. 6. Surface profile and computed bedrock profile along the center line of Glacier AX010

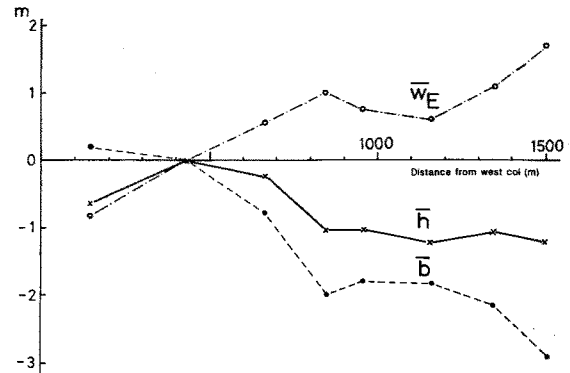


Fig. 7. Emergence flow (\bar{w}_E), net balance (\bar{b}) and ice thickness change (\bar{h}) of Glacier AX010 from Sep., 1978 to Sep., 1979

usually larger than the mean velocity with depth, the computed \bar{H} in this report is smaller than the real mean thickness.

The surface profile along the center line and the computed bedrock profile using the above \bar{H} from the west col to the terminus are shown in Fig. 6. The mean ice thickness is calculated to be 60–70 m in the upper part. The bedrock shows a convex profile where crevasses are developed in the area around surface altitudes of 5100 m–5200 m. And the ice thickness shows a minimum of 35–40 m at the steep slope, slightly increases to 45 m in the lower part, then decreases toward the terminus.

4.2. Change of ice thickness

Ice thickness change can be obtained from equation (3), ignoring melting at the glacier bed. The emergence flow and the net balance averaged over each 40 m in altitude from September 1978 to September 1979 are plotted in Fig. 7. Calculated results of ice thickness change are also shown in Fig. 7.

As clearly seen in Fig. 7, thinning of ice thickness occurred in the whole glacier, especially in the ablation area. The area-averaged thinning of the whole glacier was computed to be 0.61 m during the above period; this thinning is equivalent to 0.52 m in water equivalent, assuming the mean density of the glacier ice to be 850 kg/m^3 . This value coincides well with -0.53 m , which is the area-averaged net balance obtained from mass balance measurements during the same period (Ageta, 1983).

5. Concluding remarks

The calculated results of ice flux and change of ice thickness coincided well with the observed results of mass balance, and thinning was found over the whole glacier. Since variations of climate, glacier mass balance and ice flow are closely related, the results of field observations on Glacier AX010 may provide a useful basis for further analyses of such variation processes in the Himalaya.

Acknowledgments

We wish to express our sincere gratitude to Dr. T. Ohata and Mr. Y. Tanaka for their assistance in the observations. We are also indebted to Mr. Ang J.P. Lama and other Nepalese people for their logistic support in the field.

References

1. Ageta, Y. (1983): Characteristics of mass balance of the summer-accumulation type glacier in the Nepal Himalaya I, II. *Seppyo*, **45**, 81–105 (in Japanese with English abstract).
2. Ageta, Y., Ohata, T., Tanaka, Y., Ikegami, K. and Higuchi, K. (1980): Mass balance of Glacier AX010 in Shorong Himal, East Nepal during the summer monsoon season. *Seppyo*, **41**, Special Issue, 34–41.
3. Higuchi, K. (1980): Outline of the Glaciological Expedition of Nepal (4). *Seppyo*, **41**, Special Issue, 1–4.
4. Higuchi, K., Fushimi, H., Ohata, T., Iwata, S., Yokoyama, K., Higuchi, H., Nagoshi, A. and Iozawa, T. (1978): Preliminary report on glacier inventory in the Dudh Kosi region. *Seppyo*, **40**, Special Issue, 78–83.
5. Ohata, T. and Higuchi, K. (1980): Heat balance study on Glacier AX010 in Shorong Himal, East Nepal. *Seppyo*, **41**, Special Issue, 42–47.
6. Ohata, T., Ikegami, K. and Higuchi, K. (1980): Albedo of Glacier AX010 during the summer season in Shorong Himal, East Nepal. *Seppyo*, **41**, Special Issue, 48–54.
7. Tanaka, Y., Ageta, Y. and Higuchi, K. (1980): Ice temperature near the surface of Glacier AX010 in Shorong Himal, East Nepal. *Seppyo*, **41**, Special Issue, 55–61.